Crystal and Molecular Structure of the Ternary Complex Bis[(adenosine 5′-triphosphato)(2,2′-bipyridine)zinc(II)] Tetrahydrate

P. Orioli,*[1a] R. Cini,[1a] D. Donati,[1b] and S. Mangani[1a]

Contribution from the Istituto di Chimica Generale and the Istituto di Chimica Organica dell'Università di Siena, 53100 Siena, Italy. *Received September 17, 1980*

Abstract: The crystal structure of the dimeric species $[Zn(II)-H_2ATP-2,2'-bpy]_2 \cdot 4H_2O$ has been determined by X-ray diffraction. Cell constants are $a = 11.105$ (3), $b = 25.223$ (7), $c = 10.539$ (3) Å, $\beta = 91.34$ (4)°, with monoclinic space group $P2_1$. Diffractometer collected reflections (1617) were used for the structure determination and refinement ($R = 0.098$). The structure of the compound consists of dimeric molecules in which two zinc atoms are held together by two –OPO– bridges from the γ-phosphate groups of two ATP molecules. Both zinc atoms show a distorted octahedral coordination formed by two oxygen atoms from different γ-phosphate groups, one oxygen atom from the β-phosphate group, and the two nitrogen atoms of the bipyridyl ligand. The sixth position is filled by a α-phosphate oxygen atom which is more weakly bound. The five closest Zn–N and Zn–O distances average respectively 2.14 (4) and 2.03 (3) Å. Both ribose rings show the common C3′ endo configuration. The conformation around the exocyclic C4′–C5′ bond is gauche$^+$ for both rings. The structure is held together by strong intermolecular bipyridyl–purine and bipyridyl–bipyridyl stacking interactions. Weaker bipyridyl–purine intramolecular stacking is also observed. The molecule provides a possible model for ATP transport and phosphate group transfer mechanism.

In spite of the growing interest of crystallographers in the X-ray structure determination of transition-metal nucleotide complexes, all the structures so far reported include only monophosphate complexes.[2] Explanation for the lack of di- and triphosphate structures must be sought not only in the difficulty of getting crystalline materials, but also in the fact that most divalent metal ions catalyze the nonenzymatic transfer of phosphate from nucleoside polyphosphates to various acceptors.[3] Evaporation of solutions of the metal salts and the nucleoside polyphosphates leaves usually a mixture of metal phosphates and nucleoside monophosphate metal complexes.

Sigel and co-workers have shown that the presence of a second ligand such as bipyridyl, phenantroline, and imidazole reduces the metal-ion-promoted dephosphorylation,[4a] owing to the formation of very stable ternary complexes[4b] between the nucleoside triphosphate, the metal ion, and the second ligand.[4c] Ternary complexes involving ATP[5] have been the object of extensive investigations in solution, but very few reports have appeared concerning their characterization in the solid state.[6] The wide interest of investigators in these complexes arises essentially from two reasons: (a) they form good models for the study of the mechanism of enzymatic transfer of phosphoryl groups, since it has been shown that most of these reactions proceed through the formation of enzyme–metal–ATP complexes;[7] (b) they have been implicated in the storage and transport of ATP through membranes, because of their inactivity toward hydrolysis.[8]

The apparent contrast between the two roles can be accounted for by slight changes in the conformation of the complex molecules, as will be discussed later.

Table I. Crystal Data for $[Zn(II)-H_2ATP-2,2'-bpy]_2 \cdot 4H_2O$: $C_{40}H_{52}N_{14}O_{30}P_6Zn_2$

$a = 11.105$ (3) Å	μ(Mo Kα) = 10.46 cm^{-1}
$b = 25.223$ (7) Å	$M_r = 1525.5$
$c = 10.539$ (3) Å	$d_c = 1.74$ g/mL
$\beta = 91.34$ (4)°	$d_m = 1.74$ g/mL
V = 2951.2 Å^3	$R = 0.098$
$Z = 2$	$R_w = 0.104$
space group: $P2_1$	

We have reported the isolation of microcrystalline compounds between ATP, bipyridyl, and some 3d metal ions, such as Mn(II), Co(II), Cu(II), and Zn(II) in 1:1:1 ratio.[9] Their X-ray powder patterns are almost identical, showing them to have essentially the same structure. Small deviations, however, can be noted in the copper(II) complex diagram.

A preliminary note on the crystal and molecular structure of the zinc(II) complex has been also reported.[10] We wish to report here a detailed description of the X-ray structure of this compound.

Experimental Section

Crystals of the compound can be prepared by mixing a 10^{-3} M aqueous solution of $ZnSO_4$ (Erba, Milan) with a 50% aqueous ethanol solution of 10^{-3} M disodium adenosine 5′-triphosphate (Sigma, St. Louis) and of 2,2′-bipyridyl (Sigma) and adjusting the pH of the solution to a value of 4 with H_2SO_4. Small transparent plates form overnight, which can be filtered and washed with cold water. Under the microscope the crystals show the presence of solid deposits upon their surfaces and of large mechanical deformities.

Data Collection. A sufficiently clean crystalline fragment with approximate dimensions of $0.1 \times 0.1 \times 0.02$ mm^3 was selected and mounted on a Philips automatic diffractometer. The unit-cell parameters and other crystal data are reported in Table I.

$P2_1/m$ space group was excluded on the basis of the presence of an optically active ribose in the compound. Mo Kα radiation ($\lambda = 0.7093$ Å), monochromatized by means of a flat graphite crystal, was used to measure the intensities of 2954 independent reflections in the range $6° < 2\theta < 40°$. The ω–2θ scan technique was used, with a scan speed of 0.07°/s and a scan width of 0.8° in ω. At each end of the scan range the background was counted half of the total scan time. The reflections 041, 031, and 04$\bar{1}$, monitored periodically during data collection, did not show any systematic variation in their intensity. A total of 1617 reflections with intensity greater than $2\sigma(I)$ were considered observed and

(1) (a) Istituto di Chimica Generale; (b) Istituto di Chimica Organica.
(2) (a) Swaminathan, V.; Sundaralingam, M. *CRC Crit. Rev. Biochem.* **1979**, *6*, 245. (b) Gellert, R. W.; Bau, R. "Metal Ions in Biological Systems"; Sigel, H. Ed.; Marcel Dekker: New York, 1979; Vol. 8. (c) Hodgson, D. J. *Prog. Inorg. Chem.* **1977**, *23*, 211.
(3) Tetas, M.; Lowenstein, J. M. *Biochemistry* **1963**, *2*, 350.
(4) (a) Buisson, D. H.; Sigel, H. *Biochim. Biophys. Acta*, **1974**, *343*, 45; (b) Sigel, H. "Metal Ions in Biological Systems"; Sigel, H., Ed.; Marcel Dekker: New York, 1973; Vol. 2, p 63; (c) Sigel, H. *J. Inorg. Nucl. Chem.* **1977**, *39*, 1903.
(5) Abbreviations: bpy, 2,2′-bipyridyl; dpa, 2,2-dipyridylamine; AMP, CMP, IMP, and UMP are the 5′-monophosphates of adenosine, cytidine, inosine, and uridine, respectively; ATP, adenosine 5′-triphosphate.
(6) Cornelius, R. D.; Hart, P. A.; Cleland, W. W. *Inorg. Chem.* **1977**, *16*, 2799.
(7) Spiro, T. G. "Inorganic Biochemistry"; Eichhorn, G. L., Ed., Elsevier: New York, 1973; Vol. 1.
(8) Martin, R. P.; Scharff, J. P. "An Introduction to Bio-Inorganic Chemistry"; Williams, D. R., Ed.; Charles C. Thomas: Springfield, IL, **1976**.
(9) Cini, R.; Orioli, P. *J. Inorg. Biochem.* **1981**, *14*, 95.
(10) Orioli, P.; Cini, R.; Donati, D.; Mangani, S. *Nature* (London) **1980**, *283*, 691.

0002-7863/81/1503-4446$01.25/0

Table II. Positional Parameters (×10^4), Thermal Parameters[a] (Å^2 × 10^3), and Estimated Standard Deviations for the Atoms of [Zn(II)-H_2ATP-2,2'-bpy]$_2$·4H_2O

atom	x/a	y/b	z/c	U_{11}	U_{22}	U_{33}	U_{12}	U_{13}	U_{23}
Zn A	−4785 (5)	−801	2433 (6)	12 (3)	36 (4)	49 (5)	3 (3)	−5 (3)	0 (4)
Zn B	−1329 (5)	−1386 (3)	−178 (6)	18 (3)	45 (4)	53 (6)	−1 (3)	−5 (3)	−12 (4)

	A				B			
atom	x/a	y/b	z/c	U	x/a	y/b	z/c	U
P1	−3625 (13)	−168 (6)	5426 (16)	39 (4)	−2512 (12)	−1892 (6)	−3030 (15)	34 (4)
P2	−2482 (13)	−58 (6)	2980 (16)	36 (4)	−3635 (12)	−2129 (6)	−643 (14)	30 (4)
P3	−2028 (11)	−1206 (5)	2704 (13)	24 (4)	−4097 (13)	−986 (6)	−424 (16)	39 (5)
O5′	−4446 (28)	315 (13)	5161 (32)	36 (10)	−1745 (29)	−2398 (14)	−3172 (33)	38 (10)
O1′	−6063 (27)	1204 (12)	5715 (32)	31 (9)	−599 (26)	−2997 (12)	−5151 (30)	27 (9)
O2	−3138 (31)	−187 (15)	6688 (38)	55 (11)	−3171 (28)	−1772 (13)	−4279 (32)	42 (10)
O2′	−5962 (38)	1874 (17)	8032 (42)	78 (14)	793 (30)	−3957 (14)	−4459 (35)	50 (11)
O3	−4402 (31)	−598 (14)	4937 (37)	50 (11)	−1833 (29)	−1479 (14)	−2387 (33)	40 (10)
O3′	−3782 (53)	1231 (25)	8118 (59)	134 (21)	−429 (30)	−3718 (15)	−2273 (35)	56 (11)
O4	−2542 (28)	−40 (13)	4520 (33)	33 (9)	−3584 (26)	−2109 (13)	−2194 (31)	30 (8)
O5	−1745 (35)	408 (18)	2593 (41)	58 (13)	−4317 (33)	−2588 (15)	−439 (38)	55 (12)
O6	−3721 (29)	−116 (13)	2462 (31)	31 (9)	−2372 (38)	−2055 (17)	−100 (42)	66 (14)
O7	−1688 (29)	−591 (13)	2789 (34)	39 (10)	−4323 (27)	−1604 (12)	−328 (31)	26 (9)
O8	−1586 (32)	−1414 (16)	4112 (35)	54 (11)	−4450 (29)	−860 (14)	−1827 (35)	52 (10)
O9	−3339 (26)	−1289 (13)	2520 (30)	29 (9)	−2756 (26)	−911 (13)	−172 (30)	33 (9)
O10	−1161 (32)	−1430 (15)	1725 (35)	51 (11)	−4957 (29)	−721 (14)	547 (32)	39 (10)
N1	−10891 (38)	159 (19)	7027 (45)	43 (13)	4577 (37)	−1973 (17)	−4444 (41)	38 (13)
N3	−9545 (33)	914 (16)	7178 (38)	34 (11)	3287 (39)	−2759 (18)	−4611 (43)	46 (13)
N6	−10240 (34)	−709 (18)	6442 (39)	41 (12)	3728 (37)	−1100 (17)	−4109 (43)	41 (13)
N7	−7893 (34)	−205 (15)	6358 (39)	35 (11)	1310 (32)	−1660 (15)	−4386 (37)	24 (10)
N9	−7459 (32)	664 (15)	6698 (36)	32 (10)	1148 (34)	−2531 (15)	−4761 (39)	33 (11)
N10	−6039 (29)	−1440 (15)	2527 (34)	26 (10)	−183 (39)	−674 (18)	−258 (43)	39 (13)
N11	−6441 (37)	−423 (17)	2905 (43)	38 (12)	376 (39)	−1710 (18)	−487 (43)	34 (13)
C1′	−6836 (45)	1170 (22)	6707 (56)	49 (15)	718 (42)	−3089 (20)	−5092 (50)	30 (14)
C2	−10627 (36)	654 (16)	7199 (42)	17 (11)	4413 (52)	−2509 (24)	−4675 (59)	64 (18)
C2′	−5946 (54)	1251 (25)	8092 (62)	67 (19)	893 (37)	−3449 (17)	−3885 (44)	15 (12)
C3′	−4876 (49)	1010 (22)	7442 (56)	53 (17)	−190 (49)	−3287 (22)	−3055 (58)	50 (16)
C4	−8679 (49)	593 (21)	6825 (55)	45 (15)	2424 (35)	−2427 (16)	−4575 (41)	2 (11)
C4′	−4836 (40)	1221 (19)	6150 (50)	28 (14)	−1259 (59)	−3249 (27)	−4255 (66)	69 (21)
C5	−8855 (34)	2 (16)	6655 (41)	12 (11)	2428 (38)	−1855 (17)	−4530 (44)	16 (12)
C5′	−3943 (42)	898 (19)	5302 (49)	34 (14)	−2194 (67)	−2852 (31)	−3596 (73)	99 (24)
C6	−10046 (60)	−251 (29)	6786 (66)	76 (21)	3580 (45)	−1667 (21)	−4212 (52)	36 (14)
C8	−6968 (68)	205 (32)	6397 (77)	97 (27)	561 (43)	−2049 (21)	−4694 (49)	37 (14)
C9	−5796 (40)	−1946 (18)	2416 (47)	26 (14)	−506 (49)	−205 (23)	−53 (57)	38 (17)
C10	−6692 (49)	−2382 (21)	2197 (54)	50 (16)	349 (52)	185 (23)	179 (59)	42 (19)
C11	−7789 (74)	−2248 (31)	2118 (79)	99 (26)	1491 (39)	92 (17)	20 (47)	28 (12)
C12	−8133 (47)	−1679 (21)	2335 (55)	36 (16)	2058 (59)	−404 (26)	−464 (65)	86 (20)
C13	−7122 (34)	−1285 (16)	2662 (40)	14 (11)	1035 (69)	−818 (33)	−424 (74)	90 (24)
C14	−7444 (44)	−758 (22)	2856 (49)	30 (14)	1253 (48)	−1377 (24)	−676 (52)	45 (16)
C15	−8569 (49)	−547 (22)	3021 (58)	44 (17)	2380 (44)	−1614 (20)	−921 (52)	32 (15)
C16	−8575 (54)	12 (26)	3221 (62)	65 (19)	2594 (49)	−2090 (24)	−908 (57)	47 (17)
C17	−7686 (59)	329 (26)	3054 (65)	70 (21)	1693 (40)	−2449 (18)	−1087 (46)	26 (13)
C18	−6494 (46)	74 (22)	2888 (56)	38 (15)	533 (38)	−2234 (18)	−733 (46)	24 (13)
OW1	−870 (70)	−2613 (31)	2055 (80)	168 (31)	−5194 (65)	452 (31)	274 (72)	147 (26)
OW2	−2712 (86)	1109 (41)	700 (95)	249 (40)	−1627 (91)	−3452 (40)	−232 (96)	236 (42)

[a] Anisotropic thermal factors are of the form $\exp[-2\pi^2(\Sigma_{i=1}^{3}\Sigma_{j=1}^{3}h_ih_ja_i^*a_j^*U_{ij})]$.

used for the structure solution and refinement. The standard deviation of an intensity was calculated as follows:

$$\sigma(I) = [P + B_1 + B_2 + (0.01I)^2]^{1/2}$$

where P is the total integrated peak count, B_1 and B_2 are the background counts, $I = P - (B_1 + B_2)$ and $0.01I$ is an empirical correction for unrealistically small standard deviations in strong reflections. Intensities were corrected for Lorentz-polarization effects; absorption effects were neglected because of the difficulty of obtaining an accurate description of the crystal shape.

Structure Solution and Refinement. The structure was solved by means of Patterson and electron-density syntheses which showed all the non-hydrogen atoms with the exception of the water oxygen atoms. In the polar space group $P2_1$ there are two possible solutions to the structural problem, differing in the sign of the y coordinate. The choice between the two possible enantiomeric structures was made on the basis of the known absolute configuration of D-ribose.

A series of full-matrix least-squares cycles with isotropic temperature factors for all the atoms reduced the agreement index R to 0.120. The y coordinate of ZnA was not refined, to fix the origin of the space group. The function minimized was $\sum w(|F_o| - |F_c|)^2$ with weights $w = 1.0/(\sigma^2(F) + 0.01F^2)$.

At this point a difference electron density synthesis was calculated, and the four highest peaks were attributed to the oxygen atoms of four water molecules although their height was lower than expected for oxygen atoms. This seemed to indicate some disorder in the distribution of the water molecules in the lattice and was confirmed by the subsequent least-squares refinement which resulted in abnormally high temperature factors for these oxygen atoms. Two more least-squares cycles with the contribution of the water oxygen atoms and with allowance for anisotropic motion of the zinc atoms gave final R and R_w factors of 0.098 and 0.104, respectively. R_w is defined as $[\sum w(|F_o| - |F_c|)^2/\sum wF_o^2]^{1/2}$.

All the calculations were performed with the set of programs SHELX-76,[11] which use the analytical approximation for the atomic scattering factors and anomalous dispersion corrections for all the atoms taken from the International Tables.[12]

Table II reports the list of the final atomic coordinates and thermal parameters with estimated standard deviations obtained from the least-squares calculations. A table of observed and calculated structure factors

(11) Sheldrick, G. M. "SHELX-76. 1976 Program for Crystal Structure Determination"; Cambridge University.
(12) "International Tables for X-Ray Crystallography"; Kynoch Press: Birmingham, England, 1974; Vol. 4.

Table III. Bond Lengths (Å) and Angles (deg) around the Zinc Atoms and in the Phosphate Chains with Estimated Standard Deviations in Parentheses

metal coordination				triphosphate	A	B
ZnA-O3A	2.71 (4)	ZnB-O3B	2.39 (3)	P1-O5′	1.54 (3)	1.54 (3)
ZnA-O6A	2.09 (3)	ZnB-O6B	2.05 (4)	P1-O2	1.42 (4)	1.52 (3)
ZnA-O9A	2.02 (3)	ZnB-O9B	2.00 (3)	P1-O3	1.47 (3)	1.45 (3)
ZnA-O10B	2.00 (3)	ZnB-O10A	2.01 (4)	P1-O4	1.59 (3)	1.59 (3)
ZnA-N10A	2.13 (3)	ZnB-N10B	2.20 (4)	P2-O4	1.63 (4)	1.64 (3)
ZnA-N11A	2.14 (4)	ZnB-N11B	2.09 (4)	P2-O5	1.49 (4)	1.40 (4)
				P2-O6	1.48 (3)	1.51 (4)
O3A-ZnA-O6A	76 (1)	O3B-ZnB-O6B	81 (1)	P2-O7	1.62 (3)	1.57 (3)
O3A-ZnA-O9A	88 (1)	O3B-ZnB-O9B	84 (1)	P3-O7	1.60 (3)	1.58 (3)
O3A-ZnA-O10B	163 (1)	O3B-ZnB-O10A	168 (1)	P3-O8	1.64 (4)	1.55 (3)
O3A-ZnA-N10A	100 (1)	O3B-ZnB-N10B	99 (1)	P3-O9	1.48 (3)	1.52 (3)
O3A-ZnA-N11A	79 (1)	O3B-ZnB-N11B	90 (1)	P3-O10	1.54 (4)	1.57 (3)
O6A-ZnA-O9A	93 (1)	O6B-ZnB-O9B	93 (1)			
O6A-ZnA-O10B	88 (1)	O6B-ZnB-O10A	87 (1)	O5′-P1-O2	114 (2)	110 (2)
O6A-ZnA-N10A	173 (1)	O6B-ZnB-N10B	179 (2)	O5′-P1-O3	100 (2)	111 (2)
O6A-ZnA-N11A	97 (1)	O6B-ZnB-N11B	101 (2)	O5′-P1-O4	100 (2)	101 (2)
O9A-ZnA-O10B	99 (1)	O9B-ZnB-O10A	95 (1)	O2-P1-O3	121 (2)	120 (2)
O9A-ZnA-N10A	93 (1)	O9B-ZnB-N10B	88 (1)	O2-P1-O4	107 (2)	101 (2)
O9A-ZnA-N11A	161 (1)	O9B-ZnB-N11B	164 (1)	O3-P1-O4	113 (2)	112 (2)
O10B-ZnA-N10A	94 (1)	O10A-ZnB-N10B	92 (1)	P1-O4-P2	130 (2)	127 (2)
O10B-ZnA-N11A	97 (1)	O10A-ZnB-N11B	94 (1)	O4-P2-O5	107 (2)	102 (2)
N10A-ZnA-N11A	76 (1)	N10B-ZnB-N11B	78 (2)	O4-P2-O6	108 (2)	109 (2)
ZnA-O3A-P1A	124 (2)	ZnB-O3B-P1B	129 (2)	O4-P2-O7	100 (2)	102 (2)
ZnA-O6A-P2A	127 (2)	ZnB-O6B-P2B	127 (2)	O5-P2-O6	119 (2)	123 (2)
ZnA-O9A-P3A	134 (2)	ZnB-O9B-P3B	135 (2)	O5-P2-O7	108 (2)	113 (2)
ZnA-O10B-P3B	124 (2)	ZnB-O10A-P3A	127 (2)	O6-P2-O7	112 (2)	105 (2)
ZnA-N10A-C9A	126 (3)	ZnB-N10B-C9B	126 (4)	P2-O7-P3	133 (2)	138 (2)
ZnA-N10A-C13A	113 (3)	ZnB-N10B-C13B	110 (4)	O7-P3-O8	101 (2)	103 (2)
ZnA-N11A-C14A	114 (3)	ZnB-N11B-C14B	117 (3)	O7-P3-O9	112 (2)	106 (2)
ZnA-N11A-C18A	119 (3)	ZnB-N11B-C18B	122 (3)	O7-P3-O10	104 (2)	106 (2)
				O8-P3-O9	110 (2)	111 (2)
				O8-P3-O10	108 (2)	113 (2)
				O9-P3-O10	119 (2)	116 (2)

is available as supplementary material (see paragraph at the end of the paper).

Inspection of Table II shows that standard deviations of the atomic parameters are particularly large and prevent a detailed discussion of the bond lengths and angles. We discuss briefly the sources of errors in the present structure and point out that some of them are experimental, but others are inherent to the peculiarity of the structure itself. The main source of experimental errors is undoubtedly the low ratio between the number of observed intensities and the number of parameters, which amounts only to 1617/378 = 4.3. Trials to grow larger and better crystals for collection of data have failed so far. Other sources of errors are the uncorrected absorption effects and the neglected contribution of the 52 hydrogen atoms. However, a remarkable contribution to the large standard deviations of the atomic parameters derives from the polar nature of the structure and from the presence of a striking pseudocentrosymmetry. It has been shown, in fact, that polarity and pseudosymmetry cause large correlation between atomic parameters which sometimes can cause difficulties in the refinement process (oscillations of the calculated shifts, negative temperature factors, etc.) but always will result in large standard deviations on the structural parameters.[13]

Finally, the presence of the disordered water molecules in the crystal lattice is an additional source of difficulties, which prevent a more accurate description of the model.

However we believe that the reported standard deviations, calculated from the least-squares cycles, are close to the true values, and this is confirmed by comparison with standard deviations calculated by averaging chemically equivalent bonds.

Discussion

Description of the Structure. The structure of the compound consists of dimeric molecules in which two zinc atoms are held together by two –OPO– bridges from the γ-phosphate groups of two ATP moieties (Figure 1). Bond distances and angles around the metal atoms and in the phosphate chains are listed in Table III. Bond lengths and angles in the rest of the molecule, as well as equations of the most significant least-squares planes, are available (supplementary material). Both zinc atoms show a 5 + 1 type coordination, formed by two oxygen atoms from two different γ-phosphate groups, one β-oxygen atom, and the two nitrogen atoms of the bipyridyl group. An α-oxygen atom at a greater bond distance completes a distorted octahedral coordination. There is an approximate noncrystallographic center of symmetry which relates most of the atoms of the two monomers. The largest deviations from centrosymmetry are obviously shown by the ribose atoms.

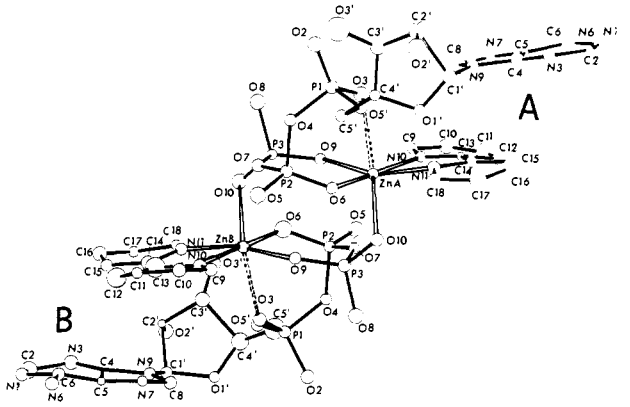

Figure 1. ORTEP drawing of the dimeric molecule of [Zn(II)–H_2ATP-2,2′-bpy]$_2$, showing also the labeling of the atoms.

In both independent ATP molecules, the phosphate chain folds back, so that the adenine moieties can stack with the bipyridyl ligand within the same dimer (see later).

Within the crystal, the dimers are held together by a complex system of stacking interactions and hydrogen bonds, which is discussed later. The water molecules are distributed in the lattice with some degree of disorder and take part in the hydrogen-bonding network.

The two zinc atoms within a dimer and the two bridging γ-phosphate groups form an eight-membered puckered ring, which

(13) (a) Templeton, D. H. *Z. Kristallogr.* **1960**, *113*, 234; (b) Lingafelter, E. C.; Orioli, P.; Schein, B. J. B.; Stewart, J. M. *Acta Crystallogr.* **1960**, *20*, 451.

Table IV. Phosphate Chain Torsion Angles in Degrees (the Estimated Standard Deviation Is 3° for Each Angle[a])

angle	molecule A	molecule B
C3'-C4' → C5'-O5'	64	54
C4'-C5' → O5'-P1	−130	154
C5'-O5' → P1-O2	60	−53
→ P1-O3	−169	172
→ P1-O4	−54	53
O5'-P1 → O4-P2	−71	89
O2-P1 →	169	−158
O3-P1 →	35	−29
P1-O4 → P2-O5	141	−147
→ P2-O6	11	−16
→ P2-O7	−106	95
O4-P2 → O7-P3	85	−66
O5-P2 →	−163	−176
O6-P2 →	−29	47
P2-O7 → P3-O8	−104	83
→ P3-O9	14	−34
→ P3-O10	144	−158

[a] Conventions on signs for the angles as in ref 2a.

is quite common in oxophosphorus complexes. This same ring, for instance, has been found in some monophosphate metal nucleotide complexes[14] and in the double bridged phosphinato complexes.[15]

The six shortest Zn–O distances aveage 2.03 ± 0.03 Å, which is somewhat longer than the Zn–O (phosphate) bond lengths found in [Zn(IMP)]$_n$[16] and [Zn(CMP)(H$_2$O)]$_n$[17]. However, it should be pointed out that in the reported cases the coordination geometry around the zinc atom is tetrahedral. The same trend is also shown by the Zn–N distances, which average 2.14 ± 0.04 Å.

The difference between the two longer Zn–O distances (2.39 and 2.71 Å) is about 10 times their standard deviation and therefore must be considered significant. It is interesting to note that the more distant oxygen atom, O3A, is also involved in a strong intermolecular hydrogen bond (2.65 Å) with an amino nitrogen atom.

The Zn–Zn distance within the dimer is 4.89 Å.

Phosphate Chains. The phosphate chains are in the folded configuration as found in Na$_2$H$_2$ATP·3H$_2$O,[18] the P–P–P angles being 94 (2)° and 87 (2)° respectively for A and B. In both structures the phosphate chain binds to the central ion with one oxygen atom from each phosphate at the corners of a triangular face of the coordination octahedron. The facial, as opposed to the meridional coordination with the bound oxygen atoms coplanar with the metal ion, which would require an extended configuration for the triphosphate chain, has been also found in Co(NH$_3$)$_3$H$_2$P$_3$O$_{10}$,[19] where again the phosphate chain is tridentate. The extended configuration has been found for the P$_3$O$_{10}^{5-}$ ion in Na$_5$P$_3$O$_{10}$[20] and in Co(NH$_3$)$_4$H$_2$P$_3$O$_{10}$,[21] where the phosphate chain behaves as bidentate.

Table IV reports the torsion angles about the bonds. It can be noted that chains A and B are almost mirror images, the corresponding torsion angles being close in magnitude but opposite in sign. This situation is obviously connected with the presence of the pseudocenter of symmetry in the dimer.

The two six-membered α,β chelate rings show a skew-boat configuration with O6, P2, O4, and P1 essentially coplanar and Zn and O3 on the same side, respectively −1.47 and −0.13 Å in ring A and 1.28 and 0.93 Å in ring B. A similar conformation has been found also in Na$_2$H$_2$ATP[18] and in Co(NH$_3$)$_4$H$_2$P$_3$O$_{10}$.[21]

The β,γ chelate rings show a somewhat different conformation. The A ring can still be described in terms of the skew-boat, with O9, P3, O7, and P2 approximately coplanar and Zn and O6 −0.41 and −0.17 Å out of the plane. The B ring, however, appears to be better described in terms of a chair conformation with O6, O9, P2, and P3 roughly coplanar and Zn and O7 respectively −0.43 and 0.35 Å out of the mean plane.[22] These configurations are stabilized by several strong hydrogen bonds involving O2, O3, O5, O8, and O10, which is discussed later.

Although a detailed discussion of the bond lengths and angles in the triphosphate chain is prevented by the large standard deviations, it can be noted that the 12 backbone P–O bonds average 1.59 (4) Å, whereas the mean of the other 12 P–O bonds is 1.49 (5) Å. Although the difference is barely significant, this behavior is in agreement with that found in linear inorganic poliphosphates[23] and in Co(NH$_3$)$_4$H$_2$P$_3$O$_{10}$[21] and is indicative of a certain degree of strain in the backbone P–O bonds. The P–O bond length in the PO$_4^{3-}$ ion, as determined by several X-ray investigations, appears to be close to 1.51 Å.[23]

Ribose. Both ribose rings in the structure show the common C3' endo conformation with deviations of C3' from the mean plane of −0.62 Å in ribose A and 0.75 Å in ribose B. The conformation around the exocyclic C4'-C5' bond is gauche$^+$ for both rings, the backbone torsion angle O5'–C5'–C4'–C3' being respectively 64° for ring A and 54° for ring B (conventions on signs and nomenclature are as in ref 2a). This configuration is similar to that found in Na$_2$H$_2$ATP and also has been observed in a number of nucleotide complexes.[2a] The glycosidic torsion angles χ O1'–C1'–N9–C4 are −132° and 179° for ring A and ring B, respectively, which corresponds to the rather common anti configuration. This angle sets the orientation of the purine moiety relatively to bipyridyl. The endocyclic torsion angles τ average 28° and 29° for ribose A and B, respectively, with a τ_{max} value of 43° for both rings.

Molecular structures of nucleotide ternary complexes with "phosphate only" metal bonding can be divided into two types depending on the intramolecular interaction between the purine moiety and the second ligand, i.e., a stacked folded and unstacked opened form.[24,25]

The type of complex formed appears essentially to be controlled by the value of the backbone torsion angle O5'–C5'–C4'–C3': gauche$^+$ conformations are responsible for folded forms, whereas trans or gauche$^-$ conformations favor opened forms. In agreement with this classification, the structure of [Zn(H$_2$ATP)(bpy)]$_2$ conforms to the folded stacked type, although intramolecular stacking interactions are not as strong as the intermolecular ones (see later).

Bipyridyl and Purine. A detailed discussion of the bond lengths and angles in the bipyridyl ligand and in the purine base is prevented by the large standard deviations on the molecular parameters. The four pyridine rings of the bipyridyl ligands are essentially planar. The metal atoms are −0.66 and 0.41 Å out of the planes defined by the pyridine rings A and B, respectively, involved in the intermolecular stacking with the purine groups (see below). The two purine rings are essentially planar.

Inter- and Intramolecular Stacking Interactions. Table V and Figures 2–5 show the complete picture of the inter- and intramolecular stacking interactions. Inspection of Table V shows that intramolecular interactions are by far the strongest ones. There are two types of intermolecular stacking interactions, i.e., a bipyridyl–purine interaction and a bipyridyl–bipyridyl self-stacking. The intramolecular interaction is of the purine–bipyridyl type via

(14) (a) Fischer, B. E.; Bau, R. *Inorg. Chem.* **1978**, *17*, 27; (b) Aoki, K. *J. Am. Chem. Soc.* **1978**, *100*, 7106.
(15) Colamarino, P.; Orioli, P.; Benzinger, W. D.; Gillman, H. D. *Inorg. Chem.* **1976**, *15*, 800.
(16) De Meester, P.; Goodgame, D. M. L.; Jones, T. J.; Skapski, A. C. *Biochim. Biophys. Acta*, **1974**, *353*, 392.
(17) Aoki, K. *Biochim. Biophys. Acta* **1976**, *447*, 379.
(18) Kennard, O.; Isaacs, N. W.; Motherwell, W. D. S.; Coppola, J. C.; Wampler, D. L.; Larson, A. C.; Watson, D. G. *Proc. R. Soc. London Ser. A*, **1971**, *325*, 401.
(19) Merritt, E. A.; Sundaralingam, M. *Abstr. Am. Crystallogr. Assoc.* **1977**, *5*, 64.
(20) Cruickshank, D. W. J. *Acta Crystallogr.* **1964**, *17*, 674.
(21) Merritt, E. A.; Sundaralingam, M.; Cornelius, R. D.; Cleland, W. W. Biochemistry **1978**, *17*, 3274.
(22) One of the referees pointed out that the most notable difference between β,γ rings and Na$_2$ATP, Co(NH$_3$)$_n$ PPP rings is that the present ones are flatter. Q = 0.261 Å in A; Q = 0.341 Å in B; Q = 0.47–0.72 Å in other structures (Q as defined by Cremer, D.; Pople, J. A. *J. Am. Chem. Soc.* **1975**, *97*, 1354.
(23) Wells, A. F. "Structural Inorganic Chemistry", 4th ed.; Clarendon Press: Oxford, 1975; p 689.
(24) Chaudhuri, P.; Sigel, H. *J. Am. Chem. Soc.* **1977**, *99*, 3142.
(25) Aoki, K. *J. Chem. Soc., Chem. Commun.* **1979**, 589.

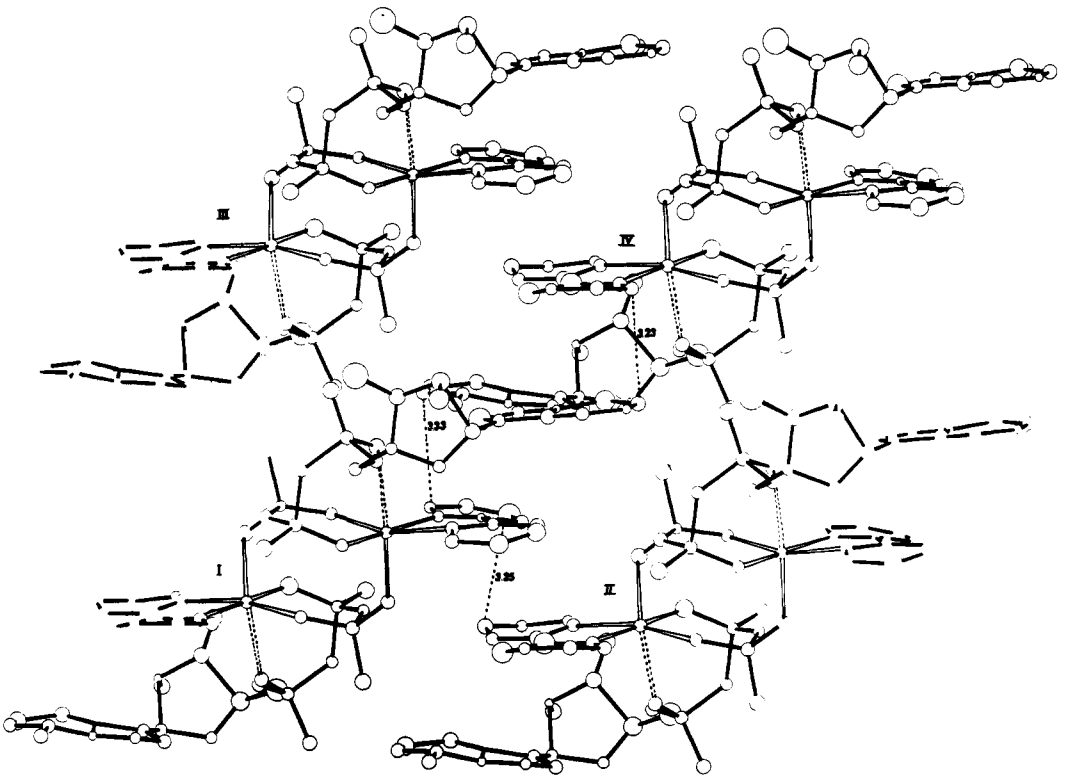

Figure 2. Diagram of four dimeric units in $[Zn(II)–H_2ATP–2,2'\text{-bpy}]_2$, showing the inter- and intramolecular stacking. The molecules are in the following positions: I (x, y, z); II $(x-1, y, z)$; III $(x, y, z+1)$; IV $(x-1, y, z+1)$. The shortest distances in the stacking sequence are also shown. Reprinted with permission from ref 8.

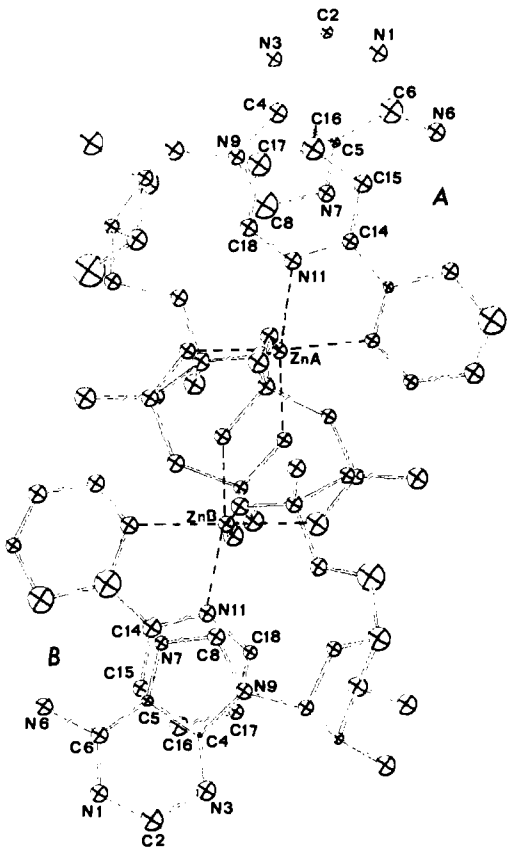

Figure 3. View of the intramolecular stacking approximately perpendicular to the planes of the aromatic rings.

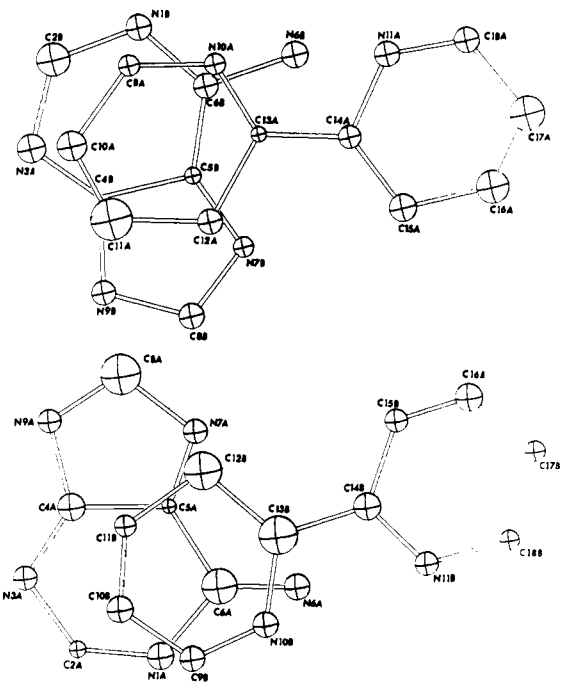

Figure 4. View of the intermolecular bipyridyl–purine stacking approximately perpendicular to the pyridine rings. Purines and bipyridyls are in the same relative positions as reported in Table V.

the metal–phosphate bridge. There are not purine–purine stacking interactions.

The stacking sequence (Figure 2) is similar to that found in $[Cu(HAMP)(bpy)(H_2O)]_2^{2+}$[14b] and consists of hydrogen-bonded adenine–adenine base pairing, intercalated between two bipyridyl ligands, which in turn are stacked on one another. The stacking sequence is therefore the following: –b–b–a:a–b–b– (b = bipyridyl and a:a = adenine–adenine base pair). Each bipyridyl ligand forms with one pyridine ring intramolecular stacking with the imidazole ring of the purine base (Figure 3) and with the other ring intermolecular stacking with the pyrimidine ring of a purine base belonging to a different molecule (Figure 4). The angles between the rings involved in the intramolecular stacking are 5° and 10°

Table V

Intermolecular Stacking Distances Shorter Than 3.60 Å

purine A–bipyridyl B (x, y, z) (x − 1, y, z + 1)	purine A–bipyridyl B (x, y, z) (x − 1, y, z + 1)	purine B–bipyridyl A (x − 1, y, z + 1) (x, y, z)	purine B–bipyridyl A (x − 1, y, z + 1) (x, y, z)	bipyridyl A–bipyridyl B (x, y, z) (x − 1, y, z)	bipyridyl A–bipyridyl B (x, y, z) (x − 1, y, z)
N1···C9 3.23	C5···C11 3.56	N1···C9 3.33	C4···C11 3.52	C10···C16 3.43	C12···C15 3.50
N1···C10 3.57	C5···C12 3.34	N1···N10 3.52	C5···C12 3.38	C11···C15 3.59	C12···N11 3.37
N7···C12 3.39	C6···C9 3.38	N3···C10 3.50	C5···C13 3.34	C11···C16 3.25	C15···C11 3.55
C2···C10 3.50	C6···C13 3.46	N7···C12 3.52	C6···C13 3.50	C11···C17 3.45	C16···C10 3.42
C4···C11 3.60	C6···N10 3.30	N9···C11 3.59	C6···N10 3.52	C11···C18 3.50	C16···C11 3.38
		C2···C9 3.38	C8···C12 3.60	C12···C14 3.32	C17···C11 3.36
		C2···C10 3.51			

Intramolecular Stacking Distances Shorter Than 4.00 Å

purine A–bipyridyl A	purine A–bipyridyl A	purine B–bipyridyl B
N7···C15 3.68	C5···C16 3.64	N7···C15 3.82
N7···C16 3.42	C8···C16 3.79	N9···C17 3.91
N7···C17 3.75	C8···C17 3.61	C5···C15 3.85
N9···C17 3.93	C8···C18 3.76	C5···C16 3.86

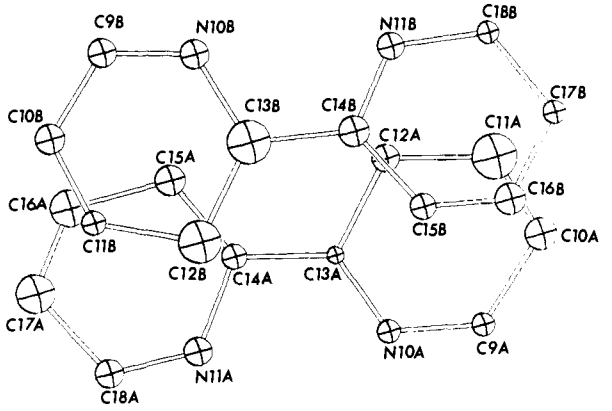

Figure 5. View of the intermolecular bipyridyl–bipyridyl stacking approximately perpendicular to the rings. The positions are as in Table V.

respectively for the A and B parts of the molecule. The intermolecular stacked rings form angles of 4° and 5° respectively for bipyridyl A and B. On the opposite side of the purine, the bipyridyl ligand stacks with another bipyridyl from a different molecule (Figure 5), the angles between the stacked pyridine rings being 9° and 13°.

Inspection of Table V shows that the two intramolecular purine–bipyridyl stacking interactions are of different strength, the purine A–bipyridyl A distances being clearly shorter than the purine B–bipyridyl B ones. It may be interesting to recall that N6 of purine B is involved in a strong intermolecular hydrogen bond with atom O3A, which probably removes the base from the best stacking position.

One interesting feature of the intramolecular stacking interaction is that it involves N7 (Figure 3 and Table V), one of the preferred binding sites in purine nucleotide complexes.[2b] N7 is also involved with N6 in hydrogen-bonded adenine–adenine base pairing (Table VI). The behavior of N7 in this compound strictly parallels that in [Cu(HAMP)(bpy)(H_2O)]$_2^{2+}$,[14b] another unusual nonbonded N7 purine nucleotide complex.

It should be noted that the crystal is formed by two sets of similar stacked molecules, which are related through the screw axis. The two sets are held together by strong hydrogen bonds (see below); there are no stacking interactions between the molecules of the two sets.

Hydrogen Bonds. Table VI shows the intra- and intermolecular hydrogen bonds in [Zn(H_2ATP)(bpy)]$_2$ as well as those involving the water molecules. It can be noted that all the nonbridging oxygen atoms of the phosphate chain are involved in hydrogen bonding.

Atom O2A shows short distances from O8B in $x, y, z + 1$ and N1A in $x + 1, y, z$ (2.75 and 2.66 Å, respectively). The angle O8B–O2A–N1A is 127°. It appears, therefore, that O2A is involved in two hydrogen bonds with O8B and N1A.

Table VI. Some Significant Hydrogen Bond Distances (Å)

O2A···N1A	$(x - 1, y, z)$	2.66
O2A···O8B	$(x, y, z + 1)$	2.75
O3A···N6B	$(x - 1, y, z + 1)$	2.65
O5A···O2'B	$(\bar{x}, {}^1/_2 + y, \bar{z} + 1)$	2.73
N6A···N7B	$(x - 1, y, z + 1)$	3.09
O8A···O2B	$(x, y, z + 1)$	2.63
O2B···N1B	$(x - 1, y, z)$	2.55
O3B···N6A	$(x + 1, y, z - 1)$	2.92
O5B···O2'A	$(\bar{x} - 1, y - {}^1/_2, \bar{z} + 1)$	2.89
N6B···N7A	$(x + 1, y, z - 1)$	2.93
OW1A···O10A	(x, y, z)	3.02
OW2A···O3'A	$(x, y, z - 1)$	2.96
OW2A···O5A	(x, y, z)	2.86
OW1B···O10B	(x, y, z)	2.98
OW2B···O3'B	(x, y, z)	2.64

The same situation holds for atom O2B, with short distances from O8A in $x, y, z - 1$ and N1B in $x - 1, y, z$ (2.63 and 2.55 Å, respectively) and an angle O8A–O2B–N1B of 133°. This obviously implies that the two residual protons of H_2ATP are bound to O8 and N1. This is also in agreement with the results from solution studies.[24]

Other interesting hydrogen bonds are those between the ribose oxygen atoms O2', A and B, with O5, B and A, respectively, which connect molecules related by the screw axis.

The amino atom N6 forms intermolecular hydrogen bonds with O3 and with N7 (Table VI). Of these bonds, the one connecting N6B and O3A appears particularly strong (2.65 Å) and has been already related with the loosening of the ZnA–O3A bond in comparison with ZnB–O3B. The water molecules are involved in a complicated network of intra- and intermolecular hydrogen bonds with the ribose oxygen O3' and the phosphate oxygen atoms O5 and O10.

Solution Studies. It cannot be stated whether the structure of [Zn(H_2ATP)(bpy)]$_2$ found in the solid state persists also in aqueous solution. Evidence has been reported[9] that the visible reflectance spectrum of the cobalt isomorphous compound does not change in solution. This only means, however, that the stereochemistry around the metal atom remains unaltered, but nothing can be said about the presence of dimeric molecules in solution. Molecular weight measurements have not been performed owing to the low solubility of the complex in all solvents. It should be pointed out that in the solid state the dimeric structure with –OPO– bridges is particularly stable and has been found in a number of nucleotide complexes.[14,25,26]

(26) Aoki, K. *J. Chem. Soc., Chem. Commun.* **1977**, 600.

The stability toward hydrolysis of ATP ternary complexes has been investigated by Sigel and co-workers,[27,28,29] who have proposed a structural model which accounts for the properties of these complexes in solution.[29] These investigations are of great importance for their biological implications, among which are (a) the mechanism of ATP transport in biological fluids and (b) the existence of ternary enzyme-metal-substrate complexes in enzyme-catalyzed dephosphorylation reactions. The crystal structure of $[Zn(H_2ATP)(bpy)]_2$ is essentially in agreement with Sigel's model:[29] (1) the chelating bipyridyl does not allow interaction of the metal ion with N7 of the base, which appears to be an essential step in the hydrolysis mechanism;[28] (2) the phosphate chain binds essentially through the β- and γ-phosphate groups, the α-phosphate group being only weakly bound; (3) a metal-ion-bridged intramolecular stacking adduct between the bipyridyl ligand and the purine base is present.

The structure of $[Zn(H_2ATP)]_2$ gives also support to the mechanism proposed for the transfer of the phosphoryl group catalyzed by those enzymes which use ATP as substrate, such as kinases.[29,30] The mechanism proposed, in fact, is based upon the possibility for the metal ion to shift from the β,γ phosphate coordination, to the α,β coordination. The present structure shows that this can be easily performed by a slight shortening of the Zn-O3 bond and consequent loosening of the Zn-O9 bond.

Supplementary Material Available: Table 1s, bond lengths in $[Zn(H_2ATP)(bpy)]_2$; Table 2s, bond angles in $[Zn(H_2ATP)(bpy)]_2$; Table 3s, least-squares plane equations; and observed and calculated factors (12 pages). Ordering information is given on any current masthead page.

(27) Sigel, H. *J. Am. Chem. Soc.* **1976**, *98*, 730.
(28) Sigel, H.; Buisson, D. H.; Prijis, B. *Bioinorg. Chem.* **1975**, *5*, 1.
(29) Sigel, H.; Amsler, P. E. *J. Am. Chem. Soc.* **1976**, *98*, 7390.
(30) Dunaway-Mariano, D.; Benovic, J. L.; Cleland, W. W.; Gupta, R. K.; Mildvan, A. S. *Biochemistry* **1979**, *18*, 4347.

Highly Selective *re* Additions to a Masked Oxaloacetate. Absolute Configurations of Fluorocitric Acids

Svante Brandänge,* Olof Dahlman, and Lars Mörch

Contribution from the Department of Organic Chemistry, Arrhenius Laboratory, University of Stockholm, S-106 91 Stockholm, Sweden. *Received December 11, 1980*

Abstract: Reformatsky reagents derived from ethyl bromofluoroacetate and ethyl 2-bromopropionate add with high selectivity (>97.5%) to the carbonyl group of **2** in a *re* (equatorial) manner, yielding **3a** + **3b** and **4a** + **4b**, respectively. The *re* stereochemistry of the former reaction was established by reductive defluorination of **3a** and **3b** to **10** with lithium triethylborohydride. Contrary to previous evidence, addition of the anion of cyanomethane to **2** also proceeds in a *re* fashion. The conformers in which the fluorine atom and the hydroxyl group at C-3 are trans predominate (>60%) in **3a** and **3b**. The Reformatsky products (e.g., **3a** and **3b**) could be degraded in a single step into substituted citric acids (e.g., **1a** and **1b**, respectively) and **2** can therefore be regarded as a masked oxaloacetate which gives highly selective *re* additions with the above reagents. Since the relative configurations of fluorocitric acids have been determined earlier, the absolute configurations of **1a** (1*R*,2*S*)[1] and **1b** (1*S*,2*S*)[1] could be assigned. The 1*R*,2*R* configuration could thus be ascribed to that isomer of fluorocitric acid which is formed in the citrate synthase reaction with fluoroacetyl-CoA.

The enzyme citrate (*si*)-synthase (EC 4.1.3.7) catalyzes the biosynthesis of citric acid from oxaloacetate and acetyl-CoA.[2] Fluoroacetyl-CoA also serves as a substrate and synthesis of fluorocitric acid[1] thus ensues.[3] A single stereoisomer of fluorocitric acid is formed[4] and this isomer is much more toxic than the other three stereoisomers. Recent evidence indicates that its main toxicity is due to an irreversible inhibition of the citrate transport in mitochondria rather than to the long-known inhibition of aconitase (EC 4.2.1.3).[5] An X-ray investigation of the racemate containing the inhibitory isomer revealed that the isomer belongs to the 1*RS*,2*RS* pair,[1,6] but the absolute configuration was not determined.[7] A biosynthesis of fluorocitric acid which proceeds with the same stereochemistry as that leading to citric acid[8] would give a fluorocitric acid with 2*R* configuration; the 1*R*,2*R* isomer (**1c**) has therefore been regarded[6a] as the probable inhibitory

Scheme I

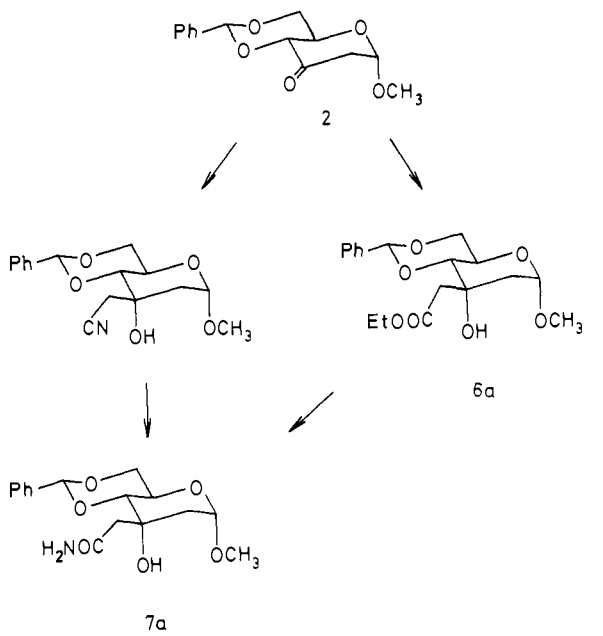

(1) The numbering of citric acid and its derivatives is that of 2-hydroxy-1,2,3-alkanetricarboxylic acids.
(2) (a) Spector, L. B. *Enzymes* **1972**, *7*, 357-368; (b) Srere, P. A. *Adv. Enzymol.* **1975**, *43*, 57-101; (c) Weitzman, P. D. J.; Danson, M. J. *Curr. Top. Cell. Regul.* **1976**, *10*, 161-204.
(3) Fanshier, D. W.; Gottwald, L. K.; Kun, E. *J. Biol. Chem.* **1964**, *239*, 425-434.
(4) Dummel, R. J.; Kun, E. *J. Biol. Chem.* **1969**, *244*, 2966-2969.
(5) (a) Kun, E.; Kirsten, E.; Sharma, M. L. *Proc. Natl. Acad. Sci. U.S.A.* **1977**, *74*, 4942-4946; (b) Kirsten, E.; Sharma, M. L.; Kun, E. *Mol. Pharmacol.* **1978**, *14*, 172-184.
(6) (a) Carrell, H. L.; Glusker, J. P.; Villafranca, J. J.; Mildvan, A. S.; Dummel, R. J.; Kun, E. *Science* **1970**, *170*, 1412-1414; (b) Carrell, H. L.; Glusker, J. P. *Acta Crystallogr., Sect. B* **1973**, *29*, 674-682.
(7) An X-ray investigation which appeared after the completion of our manuscript shows that the inhibitory isomer possesses the 1*R*,2*R* configuration: Stallings, W. C.; Monti, C. T.; Belvedere, J. F.; Preston, R. K.; Glusker, J. P. *Arch. Biochem. Biophys.* **1980**, *203*, 65-72.

0002-7863/81/1503-4452$01.25/0